The mass-number dependence studies for the multiplicity of shower particles produced in interactions of different projectiles with emulsion nuclei at 3.7 GeV/n in the framework of the modified Glauber models I and II

M.S.M. Nour El-Din and M.E. Solite

Abstract: In the present work, we calculate the total reaction cross sections for the reactions of the following projectiles: P, ^{12}C, ^{14}N, ^{16}O, ^{22}Ne, ^{24}Mg, ^{28}Si, and ^{32}S with emulsion nuclei, at incident energy E_{Lab} = 3.7 GeV/n, in the framework of the modified Glauber models I and II (Gl-I and Gl-II approaches). At the same time the number of interacted nucleons from these projectiles and the emulsion target nuclei beside the number of their binary collisions are calculated. Also the multiplicity of the shower particles produced in these reactions are calculated. A comparison between the calculated values of these total reaction cross sections and their multiplicities of the produced shower particles in these reactions, with the corresponding measured values, had been done within both: Gl-I and Gl-II approaches and in accordance to the zero-range considerations. As a result of this comparison we have not obtained an agreement between the calculated values and the corresponding experimental data in case of the total reaction cross sections, but we have got, in general, a good agreement for the comparison in the case of the particle multiplicities calculations. It should be noted, for the last comparison, that the theoretical calculations in the framework of Gl-II approach give, in general, agreement with the corresponding experimental data better than those we have obtained for the theoretical calculations in the framework of the Gl-I approach.

PACS Nos: 24.10.Cn, 24.10.Ht, 25.60.Dz

Résumé : Nous calculons ici, dans le cadre des modèles I et II modifiés de Glauber (approches Gl-I et Gl-II), les sections efficaces totales de réaction dans des collisions impliquant les projectiles suivants, P, ^{12}C, ^{14}N, ^{16}O, ^{22}Ne, ^{24}Mg, ^{28}Si et ^{32}S sur les noyaux d'une émulsion, à une énergie incidente E_{Lab} = 3,7 GeV/n. Nous calculons en même temps le nombre de nucléons qui ont interagi dans l'interaction entre les projectiles et les noyaux cibles de l'émulsion. Nous évaluons aussi la multiplicité des particules dans la gerbe produite par ces collisions. Nous avons comparé les valeurs calculées pour les sections efficaces totales de réaction et leurs multiplicités dans les gerbes produites dans ces réactions avec les valeurs mesurées correspondantes, et ce pour les deux approches Gl-I et Gl-II à portée nulle. Les sections efficaces ne montrent pas un bon accord, mais il y a un bon accord pour les multiplicités. Il faut noter pour cette dernière comparaison que les calculs dans l'approche Gl-II donnent généralement un meilleur accord que Gl-I pour les multiplicités, ce que nous observons ici.

[Traduit par la Rédaction]

1. Introduction

The heavy-ion reactions, in both the low- and high-energy domains, have been studied extensively in recent years, where it becomes an extremely interesting and promising field of nuclear research. The studying of these reactions provides quantitative consideration for the geometrical configuration of the nuclei when they collide. One of the most important theoretical models, in the last decades is the Glauber model [1], which is based on the individual nucleon–nucleon collisions in the overlap zone of the colliding nuclei. Also, one of the most fundamental quantities characterizing the heavy-ion interactions is the total reaction cross sections. This fundamental quantity has been studied, both experimentally and theoretically, for a long time [2–13].

At high energies, the Glauber model has successfully described the heavy-ion reaction cross sections. This model has been extended to study the differential elastic-scattering cross sections, the total reaction cross sections, etc.… . This extension had been done, for the low-energy domain, by modifying the model by taking into account the effect of the Coulomb field, which allows the straight-line trajectory of the colliding nuclei to be deviated [14–20]. This approach is called the Coulomb-modified Glauber model or modified Glauber model-I (Gl-I approach). Using this modified model many theoreticians had succeeded, as mentioned before, in describ-

Received 5 December 2008. Accepted 24 February 2009. Published on the NRC Research Press Web site at cjp.nrc.ca on 7 October 2009.

M.N. El-Din[1] and M. Solite. Physics Department, Faculty of Science, Benha University, Benha, Egypt.

[1]Corresponding author (e-mail: msm.nour_el_din@yahoo.com).

ing the total reactions cross sections from a few MeV/n up to a few GeV/n for several systems of colliding nuclei.

The modified Glauber model-I has been refined to take into account the nuclear potential effect on the trajectory of the scattered particle [21, 22]. This formalism is referred to as modified Glauber model-II (Gl-II approach). This new version of the Glauber model has been applied satisfactorily to elastic-scattering reactions [21]: $^{16}O + {}^{12}C$ and $^{16}O + {}^{28}Si$ at laboratory energy: $E_{Lab.} = 1503$ MeV. In addition, analytical expressions for the elastic scattering, in the reaction: $^{12}C + {}^{12}C$ at $E_{Lab.}$ running from 25 up to 342.5 MeV/n, were studied by Farag [10], using both the Gl-I and Gl-II approach. Farag concluded that both modifications can be used in the calculations of the heavy-ion elastic scattering at low energies and these modifications have improved the results of the total reactions cross sections.

Many theoreticians and experimentalists [23–32] have exerted great efforts to study the different productions in the interactions of different projectiles with the emulsion nuclei at $E_{Lab.} = 3.7$ GeV/n. It should be noted that we are interested, in the present work, in one of these different productions such as the multiplicity of the shower particles that are produced as a result of the interactions of the different projectiles considered with the emulsion nuclei.

In the present work, the total reaction cross sections, for the collision of many projectiles such as P, ^{12}C, ^{14}N, ^{16}O, ^{22}Ne, ^{24}Mg, ^{28}Si, and ^{32}S with emulsion nuclei, have been calculated, at incident energy $E_{Lab} = 3.7$A GeV/n. These calculations have been done in the framework of the Gl-I and Gl-II approaches. In addition, the number of nucleons from the interaction of the projectiles and the target

and the number of their binary collisions are evaluated. Then the corresponding multiplicity of the shower particles, which are produced in these reactions, was calculated and compared with the corresponding experimental data.

2. Formalism

According to the optical limit of the Glauber theory [17, 18], the total reaction cross section is given by the following formula:

$$\sigma_{\text{total}-r}\ (\text{mb}) = 20\pi \int b\,\mathrm{d}b[1 - T(b)] \tag{1}$$

where $T(b)$ defines the probability that at the impact parameter b, the high-energy projectile traverses the target without interaction [18] and it is known as a transparency function. This function is given by

$$T(b) = \exp\left[-2\,Im\delta(b)\right] \tag{2a}$$

where

$$\delta(b) = \frac{1}{2}\bar{\sigma}_{nn}(\alpha_{nn} + i)\chi(b) \tag{2b}$$

represents the optical nuclear phase-shift function that is given as a function in the impact parameter, b. Furthermore, $\bar{\sigma}_{nn}$ is the average energy-dependent nucleon–nucleon cross section [33], while α_{nn} is the ratio of the real to the imaginary part of the forward nucleon–nucleon amplitude.

The imaginary part of the nuclear phase-shift function, $\chi(b)$, can be calculated by the following overlap integral [17, 18, 20, 33]:

$$\chi_T(b) = \frac{1}{10}\int \mathrm{d}^2 b_T \int_{-\infty}^{\infty} \mathrm{d}z_T \rho_T(b_T, z_T) f(b_T - b) \tag{3a}$$

in case of the nucleon–nucleus interaction, while in case of the nucleus–nucleus interaction the overlap integral is given by

$$\chi_{TP}(b) = \frac{1}{10}\int \mathrm{d}^2 b_P \int_{-\infty}^{\infty} \mathrm{d}z_P \int \mathrm{d}^2 b_T + \int_{-\infty}^{\infty} \mathrm{d}z_T \rho_P(b_P, z_P)\rho_T(b_T, z_T) f[b_T - (b - b_P)] \tag{3b}$$

It should be noticed that $\rho_P(\rho_T)$ stand for the nuclear density of the projectile (target) nucleus. The f-function accounts for the finite range of the nucleon–nucleon interaction and it is, usually, given in a Gaussian form [18]

$$f(b) = \frac{1}{\pi r_0}\exp\left(\frac{b^2}{r_0^2}\right) \tag{4}$$

where the parameter r_0 is known as the nucleon–nucleon reaction range parameter.

For simplicity, the Gaussian shape for the nuclear density distribution has been adopted in the present study for both the projectile and target [2, 34]:

$$\rho_i(r_i) = \rho_i(0)\exp\left[-\frac{b_i^2 + z_i^2}{a_i^2}\right] \tag{5}$$

where $\rho_i(0)$ and a_i are the central nuclear density and the diffuseness parameter, respectively. Both of them are related to the root mean square radius, $R_{\text{rms}}^{(i)}$, through [2, 34]

$$\rho_i(0) = \frac{A_i}{(a_i\sqrt{\pi})^3} \quad \text{and} \quad a_i = \sqrt{\frac{2}{3}}R_{\text{rms}}^{(i)} \tag{6}$$

where i stands for P, T (projectile and target).

Carrying out the integrations in (3), over b_p, Z_p, b_T, and Z_T, the phase shift function $\chi(b)$, in case of the nucleon–nucleus interaction, will be [11, 18, 33, 35]

$$\chi_T(b) = \chi_{0T}\exp\left[-\frac{b^2}{a_T^2 + r_0^2}\right] \tag{7a}$$

where

$$\chi_{0T} = \frac{\bar{\sigma}_{nn}\sqrt{\pi}\rho_T(0)^T a_T^3}{10(a_T^2 + r_0^2)} \tag{7b}$$

while, in case of the nucleus–nucleus interaction, we have obtained

$$\chi_{PT}(b) = \chi_{0PT}\exp\left[-\frac{b^2}{a_P^2 + a_T^2 + r_0^2}\right] \tag{8a}$$

where

$$\chi_{0PT} = \frac{\bar{\sigma}_{nn}\pi^2\rho_P(0)\rho_T(0)a_P^3a_T^3}{10(a_P^2 + a_T^2 + r_0^2)} \tag{8b}$$

Taking into account the effect of the Coulomb field, there will be a deviation in the eikonal trajectory of the scattered particle. This situation corresponds to what is known as the Coulomb modified Glauber model (GL-I approach). This deviation is associated with what is called the closest approach distance between the interacting particles, b', which is given by [33]

$$b' = \frac{\eta + (\eta^2 + k^2b^2)^{1/2}}{k} \tag{9}$$

where k is the wave number and η is the Sommerfeld parameter.

Cha [21] suggests that the distance of the closest approach in the presence of the nuclear and the Coulomb field, can be obtained as the solution of the equation

$$1 - \frac{V_{\mathrm{eff}}(r)}{E} = 1 - \frac{2\eta}{kr} - \frac{L^2}{k^2r^2} - \frac{V_n(r)}{E} = 0 \tag{10}$$

Here, $V_{\mathrm{eff.}}(r)$ represents the total potential or what is known as the effective potential, $V_n(r)$ is the real part of the nuclear optical potential, E is the kinetic energy in center of mass system, and L is the angular momentum. The solution of (10) can be obtained in different ways. One of them is a solution when $V_n(r) = 0$, which is given by (9) as b'. The other one can be obtained if the first order for a Taylor series expansion is carried out around $r = b'$. The solution has been given by Cha [21] as

$$d = b' - \frac{\mathrm{Re}l.V_n(b')}{\mathrm{Re}l.V'_{\mathrm{eff}}(b')} \tag{11}$$

where $V'_{\mathrm{eff}}(b')$ is the derivative of $V_{\mathrm{eff}}(r)$ with respect to r and it is evaluated at $r = b'$. However, in his work, Cha used the Wood–Saxon potential version for $V_n(r)$.

Within the Glauber model, one can obtain, from the phase shift (2b), a nuclear optical potential ($V_n(r)$) according to the following integral transformation [36]:

$$V_n(r) = \frac{2\hbar v}{\pi r}\frac{\mathrm{d}}{\mathrm{d}r}\int_r^\infty \frac{\delta(b)}{(b^2 - r^2)^2}\, b\,\mathrm{d}b \tag{12}$$

It is clear, according to this equation, that the value of $V_n(r)$ receives contributions from all values of $b \geq r$. At the same time, since the considered phase shift, in the present study, is also associated with the modified trajectory (curved trajectory), given by (9), then Vitturi and Zardi [15, 16] replaced expression of $V_n(r)$, given by (12), with another one given as follows:

$$V_n(r) = \frac{2\hbar v}{\pi r}\frac{\mathrm{d}}{\mathrm{d}r}\int_r^\infty \frac{\delta(b')}{(b'^2 - r^2)^{1/2}}\, b\,\mathrm{d}b \tag{13}$$

which, only in the case of straight trajectories, coincides with (12). At variance with expression, given by (13), the values of $V_n(r)$ receive contributions from all values of the closest distance approach (b'), i.e., for all values of $b' \geq r$.

Now, in accordance to (7), (8), and (13), the nuclear optical potential, in case of the nucleon–nucleus scattering, is given by

$$[V_n(r)]_{nN} = -\frac{\hbar v\bar{\sigma}_{nn}}{10\pi}(\alpha_{nn} + i)\frac{\rho_T(0)a_T^3}{(a_T^2 + r_o^2)^{3/2}} \times \exp\left[-\frac{r^2}{a_T^2 + r_0^2}\right] \tag{14a}$$

On the other hand, the nuclear optical potential, in case of the nucleus–nucleus scattering, has been derived, also, and it is given by

$$[V_n(r)]_{NN} = -\frac{\hbar v\sqrt{\pi^3}\bar{\sigma}_{nn}}{10}(\alpha_{nn} + i)\frac{\rho_P(0)\rho_T(0)a_p^3a_T^3}{(a_p^2 + a_T^2 + r_o^2)^{3/2}} \times \exp\left[-\frac{r^2}{a_p^2 + a_T^2 + r_0^2}\right] \tag{14b}$$

It should be mentioned that we have used, during execution our derivation, the following standard integration [37]:

$$\int_u^\infty (x - u)^n\, \mathrm{e}^{-\mu x}\,\mathrm{d}x = \mu^{-n-1}\,\mathrm{e}^{-u\mu}\,\Gamma(n+1),$$
$$[u > o, \quad \mathrm{Re}n > -1, \quad \mathrm{Re}\mu > 0] \tag{15}$$

It should be mentioned that the result of the overlap integrals of the nuclear densities (3a) and (3b) are evaluated in terms of b' (9) {Gl-I} and d (11) {Gl-II} in all our calculations. Also all our calculations have been carried out taking into account, only the zero-range consideration.

Substituting (9) in (2) and (1) one can calculate $\sigma_{\mathrm{total}-r}$ for a proton and an oxygen nucleus , as projectiles, with each one of the constituents of the emulsion, respectively. These calculated cross sections have been used in the calculations of the average numbers of the projectile participants (PP) and the target participants (TP). Also, the average number of the binary-collisions (BC) has been calculated, taking into account the calculated values of $\sigma_{\mathrm{total}-r}$. The corresponding equations for PP, TP, and BC are [28]

$$<\nu_{\mathrm{PP}}> = \frac{A_P\sigma_{pA_T}}{\sigma_{A_PA_T}} \tag{16a}$$

$$<\nu_{\mathrm{TP}}> = \frac{A_T\sigma_{pA_P}}{\sigma_{A_PA_T}} \tag{16b}$$

and

$$<\nu_{\mathrm{BC}}> = \frac{A_PA_T\sigma_{\mathrm{pp}}}{\sigma_{A_PA_T}} \tag{16c}$$

respectively. It should be noted that σ_{pA_T}, σ_{pA_P}, and σ_{pp} represent the total reaction cross section of proton with a target (each element of the emulsion group will be considered as a target), a projectile (which is ^{16}O-nucleus in our study) and a proton, respectively. In addition, $\sigma_{A_PA_T}$ is the total reaction cross section of the projectile ^{16}O-nucleus, with each element of the emulsion. These calculated average numbers have, in turn, been used in the calculations of the multiplicity of the shower particles as we shall show in the next section of the results and its discussions.

3. Results and discussion

As a beginning for our discussion of the results, which have been obtained during our present study, the measured values of the rms radii of the emulsion nuclei and the corresponding chemical concentrations of these nuclei, according to the NIKFI (Br-2) type emulsion, are tabulated in Table 1. Besides this, the calculated total reaction cross sections of protons with ^{1}H-,^{12}C-,^{14}N-,^{16}O-,^{22}Ne-,^{24}Mg-,^{28}Si-,^{32}S-,^{80}Br-,^{108}Ag, ^{127}I, and ^{30}Em-target nuclei, according to the Gl-I and Gl-II approaches, are tabulated in Table 2. It should be mentioned that all our theoretical calculations are performed in accordance with the zero-range approach. Also it should be noted, in the case of the p–Em interaction that we have considered the emulsion sample as an nucleus with mass number equal 30 (^{30}Em nucleus) and its rms radius has been calculated using the following global expression of Friedrich and Voegler [38]:

$$R_{\mathrm{rms}} = 0.891A^{-1/3}(1 + 1.565A^{-2/3} - 1.04A^{-4/3}) \tag{17}$$

In Table 3, the calculated total-reaction cross sections, $\sigma^{\mathrm{theor.}}_{\mathrm{total}-r}$ and the corresponding multiplied total-reaction cross-sections, $\sigma^{\mathrm{ml.}}_{\mathrm{total}-r}$, in the framework of the Gl-I and Gl-II approaches, are tabulated for: ^{32}S-, ^{28}Si-, ^{24}Mg-, ^{22}Ne-, ^{16}O-, ^{14}N-, ^{12}C-and p–Em reactions, respectively. The multiplied total-reaction cross sections were obtained by multiplying the calculated total-reaction cross sections of the different projectiles with the individual emulsion nuclei (^{1}H ,^{12}C,^{14}N, ^{16}O, ^{32}S, ^{80}Br,^{108}Ag, and ^{127}I), with the corresponding chemical concentrations for these nuclei. It is noted, from Table 3 that the value of $\sigma^{\mathrm{theor.}}_{\mathrm{total}-r}$, which is associated with the reaction of each projectile with each separated emulsion nuclei, increases as the individual mass number of these nuclei increases. But on the other hand, one can note, for the reaction of the different projectiles with the same emulsion nucleus, that the value of $\sigma^{\mathrm{theor.}}_{\mathrm{total}-r}$, decreases as the mass number of the projectile decreases. These observations are expected where the value of the radii of both the projectile and the target play an effective role on the value of the total-reaction cross section, $\sigma_{\mathrm{total}-r}$.

Dividing the summation of $\sigma^{\mathrm{ml.}}_{\mathrm{total}-r}$, for each reaction system by the sum of the chemical concentrations of the emulsion nuclei one gets an average value for the calculated total-reaction cross sections for the different reaction systems being considered as a whole and it is denoted by $\sigma^{\mathrm{aver.}}_{\mathrm{total}-r}$. These average values are compared with the corresponding experimental data in Table 4. It is clear, from Table 4 that the values of $\sigma^{\mathrm{aver.}}_{\mathrm{total}-r}$ (Gl-II) are slightly less than that those associated with $\sigma^{\mathrm{aver.}}_{\mathrm{total}-r}$ (Gl-I). This reduction in the value of $\sigma^{\mathrm{aver.}}_{\mathrm{total}-r}$ may be due to taking into account the effect of the nuclear potential in the calculation of the total-reaction cross section. But both values of $\sigma^{\mathrm{aver.}}_{\mathrm{total}-r}$ (Gl-I) and $\sigma^{\mathrm{aver.}}_{\mathrm{total}-r}$ (Gl-II) are still in disagreement with the corresponding experimental data. This disagreement may be reduced to the smallest limit if we take into account the in-medium effect during the reaction between the nucleons of the projectile being considered and the nucleons of each individual emulsion nucleus. This effect has helped us before [11, 12, 20, 35] to refine our calculations for both the total reaction and total cross sections in such a way that, for these calculations, we got good agreement with the corresponding experimental data. Also, if we consider another nuclear distribution, especially for the emulsion nuclei ^{80}Br, ^{108}Ag, and ^{127}I, other than the Gaussian distribution form one may get better agreement between the average calculated values of the total-reaction cross sections and the corresponding experimental data.

Table 1. The rms radii of the emulsion nuclei and the corresponding chemical concentrations of these nuclei, according to the NIKFI (Br-2) type emulsion.

Chem. sym.	rms radius (fm)	Nos. atoms × 10^{22}/cc
^{1}H	0.81 [39]	2.930
^{12}C	2.442 [17]	1.390
^{14}N	2.580 [40]	0.370
^{16}O	2.710 [17]	1.060
^{32}S	3.251 [17]	0.004
^{80}Br	4.151 [38]	1.020
^{108}Ag	4.542 [17]	1.020
^{127}I	4.749 [38]	0.003

Table 2. The calculated values of the total reaction cross sections of proton with a different nuclei, in the framework of Gl-I and Gl-II approaches and their rms radii.

Reaction-systems	rms radius of the target (fm)	$\sigma^{\mathrm{theor.}}_{\mathrm{total}-r}$ (Gl-I) (mb)	$\sigma^{\mathrm{theor.}}_{\mathrm{total}-r}$ (Gl-II) (mb)
p–^{1}H	0.81 [39]	30.271	24.747
p–^{12}C	2.442 [17]	288.363	274.920
p–^{14}N	2.580 [40]	327.799	313.238
p–^{16}O	2.710 [17]	366.840	351.238
p–^{22}Ne	2.969 [40]	464.437	445.933
p–^{24}Mg	3.015 [17]	489.271	469.870
p–^{28}Si	3.096 [17]	535.423	514.369
p–^{32}S	3.251 [17]	597.712	575.168
p–^{80}Br	4.151 [38]	1110.90	1075.71
p–^{108}Ag	4.542 [17]	1375.32	1334.66
p–^{127}I	4.749 [38]	1552.30	1487.96
p–^{30}Em	3.194 [38]	571.042	549.240

It should be mentioned that the total-reaction cross sections, for the relative abundance of the different target constituents in the case of the standard nuclear emulsion have been calculated before [41]. For these calculations the following formulae have been applied:

$$\sigma_{A_{\mathrm{P}}A_{\mathrm{T}}}\ \ (\mathrm{mb}) = 109.2(A_{\mathrm{P}}^{0.29} + A_{\mathrm{T}}^{0.29} - 1.39)^2 \tag{18a}$$

$$\sigma_{\mathrm{p}A_{\mathrm{P(T)}}}\ \ (\mathrm{mb}) = 38.17A^{0.719} \tag{18b}$$

and

$$\sigma_{\mathrm{pp}}\ \ (\mathrm{mb}) = 32.3\ \ (\mathrm{mb}) \tag{18c}$$

where $\sigma_{A_{\mathrm{P}}A_{\mathrm{T}}}$, $\sigma_{\mathrm{p}A_{\mathrm{P(T)}}}$, and σ_{pp} are the reaction cross sections in the case of nucleus–nucleus, proton–nucleus, and proton–

Table 3. The average calculated values of the total reaction cross-sections of a different reaction systems, in the framework of Gl-I and Gl-II approaches, and the corresponding values of it, which are obtained according to the chemical concentrations of the emulsion nuclei in the slandered emulsion.

Element	$\sigma^{\text{theor.}}_{\text{tot.}-r.}$ (Gl-II) (mb)	$\sigma^{\text{ml.}}_{\text{tot.}-r.}$ (Gl-I) (mb)	$\sigma^{\text{theor.}}_{\text{tot.}-r.}$ (Gl-II) (mb)	$\sigma^{\text{ml.}}_{\text{tot.}-r.}$ (Gl-II) (mb)
^{32}S–Em				
^{1}H	597.712	1751.296	575.168	1685.242
^{12}C	1643.57	2284.562	1621.07	2253.287
^{14}N	1752.96	648.595	1730.83	640.407
^{16}O	1858.06	1969.544	1836.22	1946.392
^{32}S	2422.97	9.692	2402.45	9.610
^{80}Br	3552.96	3624.019	3533.15	3603.813
^{127}Ag	4102.48	4184.530	4082.64	4164.293
^{127}I	4423.87	13.272	4403.97	13.212
^{28}Si–Em				
^{1}H	535.423	1568.789	514.369	1507.101
^{12}C	1522.78	2116.664	1500.96	2086.334
^{14}N	1627.97	602.349	1606.50	594.405
^{16}O	1729.26	1833.016	1708.08	1810.565
^{32}S	2274.59	9.099	2254.61	9.018
^{80}Br	3473.78	3441.256	3353.66	3420.733
^{127}Ag	3909.61	3987.802	3890.05	3967.851
^{127}I	4223.60	12.540	4203.97	12.612
^{24}Mg–Em				
^{1}H	489.271	1433.564	469.870	1376.719
^{12}C	1436.56	1996.818	1415.22	1967.156
^{14}N	1538.45	569.227	1517.39	561.434
^{16}O	1636.56	1734.754	1615.81	1712.759
^{32}S	2166.32	8.665	2146.61	8.586
^{80}Br	3237.10	3301.842	3217.69	3282.044
^{127}Ag	3760.94	3836.159	3741.39	3816.218
^{127}I	4067.75	12.203	4048.10	12.144
^{2}Ne–Em				
^{1}H	464.437	1360.800	445.933	1306.584
^{12}C	1389.39	1931.252	1368.76	1902.576
^{14}N	1489.37	551.067	1469.05	543.549
^{16}O	1585.77	1680.912	1565.69	1659.63
^{32}S	2106.80	8.427	2087.68	8.351
^{80}Br	3161.98	3225.220	3143.05	3205.911
^{127}Ag	3678.72	3752.294	3659.61	3732.802
^{127}I	3981.49	11.944	3962.26	11.887
^{16}O–Em				
^{1}H	366.840	1074.841	351.238	1029.127
^{12}C	1193.10	1658.407	1174.94	1633.167
^{14}N	1284.50	475.08	1266.59	468.638
^{16}O	1373.66	1456.080	1355.93	1437.286
^{32}S	1858.06	7.432	1840.90	7.364

Table 3 (*concluded*).

Element	$\sigma^{\text{theor.}}_{\text{tot.}-r.}$ (Gl-II) (mb)	$\sigma^{\text{ml.}}_{\text{tot.}-r.}$ (Gl-I) (mb)	$\sigma^{\text{theor.}}_{\text{tot.}-r.}$ (Gl-II) (mb)	$\sigma^{\text{ml.}}_{\text{tot.}-r.}$ (Gl-II) (mb)
^{80}Br	2850.56	2907.571	2833.14	2889.803
^{127}Ag	3339.68	3406.474	3321.96	3388.399
^{127}I	3626.78	10.880	3608.88	10.827
^{14}N–Em				
^{1}H	327.799	960.451	313.238	917.787
^{12}C	1109.69	1542.469	1093.08	1519.381
^{14}N	1198.46	443.43	1182.05	437.359
^{16}O	1284.50	1361.57	1268.24	1344.504
^{32}S	1752.96	7.012	1737.10	6.948
^{80}Br	2718.51	2772.88	2702.18	2756.224
^{127}Ag	3195.86	3259.777	3179.18	3242.764
^{127}I	3476.28	10.429	3459.40	10.378
^{12}C–Em				
^{1}H	288.363	844.904	274.920	805.516
^{12}C	1024.58	1424.166	1008.32	1401.565
^{14}N	1109.69	410.585	1093.59	404.628
^{16}O	1192.35	1263.891	1176.35	1246.931
^{32}S	1643.57	6.574	1627.77	6.511
^{80}Br	2579.40	2630.988	2562.95	2614.209
^{127}Ag	3043.56	3104.431	3026.71	3087.244
^{127}I	3316.50	9.950	3299.43	9.892
p–Em				
^{1}H	30.271	88.695	24.747	72.507
^{12}C	288.363	400.825	274.920	382.139
^{14}N	327.799	121.286	313.238	115.898
^{16}O	366.840	388.850	351.238	372.312
^{32}S	597.712	2.391	575.168	2.301
^{80}Br	1110.90	1133.118	1075.71	1097.224
^{127}Ag	1375.32	1402.50	1334.66	1361.353
^{127}I	1552.30	4.657	1487.96	4.464

Table 4. A comparison between the average calculated values of the total-reaction cross sections of different reaction systems, in the framework of Gl-I and Gl-II approaches besides those which obtained according to (18), and the corresponding experimental data are shown in this table.

Reaction system	$\sigma^{\text{exp.}}_{\text{total}-r}$ (mb)	$\sigma^{\text{aver.}}_{\text{total}-r}$ (Gl-I) (mb)	$\sigma^{\text{aver.}}_{\text{total}-r}$ (Gl-II) (mb)	$\sigma^{\text{aver.}}_{\text{total}-r}$ (18) (mb)
^{32}S–Em	1314.0±47 [42]	1857.831	1836.124	1387.864
^{28}Si–Em	1467.0±53 [43]	1740.624	1719.715	1313.735
^{24}Mg–Em	1337.0±58 [44]	1653.614	1632.430	1234.822
^{22}Ne–Em	1294.0±39 [45]	1605.992	1586.673	1193.032
^{16}O–Em	1090.0±136 [46]	1410.384	1393.435	1055.239
^{14}N–Em	979.0 [47]	1328.462	1312.857	1003.871
^{12}C–Em	949.0±22 [48]	1243.490	1228.288	948.781

proton reactions, respectively. It should be mentioned that these formulae are valid [41] in the energy range: (2.1 → 200)A GeV. Using these formulae, the average values of the total-reaction cross sections ($\sigma^{\text{aver.}}_{\text{total}-r}$), for all the reaction systems considered are tabulated in the last column in Table 4. It is clear that for the average values ($\sigma^{\text{aver.}}_{\text{total}-r}$ (18)),

Table 5. Estimates of the amount of the nuclear matter involved in interaction of different projectiles, which are considered in this work, with the emulsion nuclei at 3.7 GeV/n are shown in this table. This estimates values are averaged over the impact parameter.

	Gl. I					Gl. II				
Element	% of reac.	$\sigma^{\text{theor.}}_{\text{tot.}-r.}$ (mb)	P.P.	T.P.	B.C.	% of reac.	$\sigma^{\text{theor.}}_{\text{tot.}-r.}$ (mb)	P.P.	T.P.	B.C.
^{32}S–Em										
^{1}H	12.090	597.71	1.62	1.00	1.62	11.772	575.17	1.38	1.00	1.38
^{12}C	15.771	1643.57	5.61	4.36	7.07	15.739	1621.07	5.43	4.26	5.86
^{14}N	4.478	1752.96	5.98	4.77	7.74	4.473	1730.83	5.79	4.65	6.41
^{16}O	13.597	1858.06	6.32	5.15	8.34	13.596	1836.22	6.12	5.01	6.90
^{32}S	0.0007	2422.97	7.89	7.89	12.79	0.0007	2402.45	7.66	7.66	10.55
^{80}Br	25.018	3552.96	10.01	13.46	21.81	25.173	3533.15	9.74	13.02	17.93
^{127}Ag	28.888	4102.48	10.74	15.74	25.50	29.088	4082.64	10.46	15.22	20.95
^{127}I	0.0009	4423.87	11.29	17.16	27.81	0.0009	4403.97	10.81	16.59	22.84
^{30}Em		2360.78	7.74	7.60	12.31		2340.17	7.51	7.37	10.15
^{28}S–Em										
^{1}H	11.559	535.42	1.58	1.00	1.58	11.240	514.37	1.35	1.00	1.35
^{12}C	15.596	1522.78	5.30	4.22	6.68	15.560	1500.96	5.13	4.11	5.54
^{14}N	4.438	1627.97	5.64	4.60	7.29	4.433	1606.50	5.46	4.48	6.04
^{16}O	13.506	1729.26	5.94	4.94	7.84	13.503	1708.08	5.76	4.82	6.49
^{32}S	0.0007	2274.59	7.36	7.53	11.92	0.0007	2254.61	7.14	7.30	9.83
^{80}Br	25.356	3373.78	8.95	12.70	20.10	25.511	3353.66	8.98	12.27	16.53
^{127}Ag	29.383	3909.61	9.85	14.79	23.41	29.592	3890.05	9.61	14.28	19.25
^{127}I	0.0009	4223.60	10.29	16.10	25.49	0.0009	4203.97	9.91	15.54	20.93
^{30}Em		2214.37	7.22	7.25	11.48		2194.30	6.97	7.03	9.47
^{24}Mg–Em										
^{1}H	11.119	489.27	1.49	1.00	1.49	10.816	469.87	1.26	1.00	1.26
^{12}C	15.487	1436.56	4.82	4.09	6.07	15.455	1415.22	4.66	3.98	5.04
^{14}N	4.415	1538.45	5.11	4.45	6.61	4.411	1517.39	4.95	4.34	5.48
^{16}O	13.455	1636.56	5.38	4.78	7.10	13.495	1615.81	5.22	4.65	5.88
^{32}S	0.0007	2166.32	6.62	7.227	10.73	0.0007	2146.61	6.43	7.00	8.85
^{80}Br	25.609	3237.10	8.24	12.09	17.95	25.786	3217.69	8.02	11.68	14.77
^{127}Ag	29.753	3760.94	8.78	14.05	20.86	29.983	3741.39	8.56	13.56	17.14
^{127}I	0.0009	4067.75	9.15	15.28	22.68	0.0011	4048.10	8.82	14.74	18.36
^{30}Em		2107.74	6.50	6.96	10.31		2087.96	6.31	6.75	8.53
^{22}Ne–Em										
^{1}H	10.867	464.44	1.43	1.00	1.43	10.561	445.93	1.22	1.00	1.22
^{12}C	15.423	1389.39	4.57	4.01	5.75	15.379	1368.76	4.42	3.91	4.77
^{14}N	4.401	1489.37	4.84	4.37	6.26	4.394	1469.05	4.69	4.25	5.19
^{16}O	13.424	1585.77	5.09	4.69	6.72	13.388	1565.69	4.94	4.56	5.56
^{32}S	0.0007	2106.80	6.24	7.05	10.12	0.0007	2087.68	6.06	6.84	8.84
^{80}Br	25.757	3161.98	7.73	11.75	16.85	25.914	3143.05	7.68	11.35	13.86
^{127}Ag	29.966	3678.72	8.23	13.64	19.55	30.173	3659.61	8.02	13.16	16.07
^{127}I	0.0009	3981.49	8.58	14.81	21.24	0.0011	3962.26	8.26	14.29	17.45
^{30}Em		2049.14	6.13	6.80	9.75		2029.96	5.95	6.590	8.05
^{16}O–Em										
^{1}H	9.774	366.84	1.32	0.95	1.32	9.7472	351.24	1.13	1.00	1.13
^{12}C	15.081	1193.10	3.87	3.67	4.87	15.032	1174.94	3.74	3.59	4.04

Table 5 (*concluded*).

	Gl. I					Gl. II				
Element	% of reac.	$\sigma_{\mathrm{tot.}-r.}^{\mathrm{theor.}}$ (mb)	P.P.	T.P.	B.C.	% of reac.	$\sigma_{\mathrm{tot.}-r.}^{\mathrm{theor.}}$ (mb)	P.P.	T.P.	B.C.
^{14}N	4.320	1284.50	4.08	4.00	5.28	4.313	1266.59	3.96	3.88	4.38
^{16}O	13.241	1373.66	4.27	4.27	5.64	13.229	1355.93	4.15	4.15	4.67
^{32}S	0.0007	1858.06	5.15	6.32	8.34	0.0007	1840.90	5.00	6.11	6.88
^{80}Br	26.440	2850.56	6.24	10.30	13.59	26.598	2833.14	6.08	9.94	11.18
^{127}Ag	30.977	3339.68	6.59	11.86	15.66	31.187	3321.96	6.43	11.42	12.87
^{127}I	0.0010	3626.78	6.85	12.85	16.96	0.0010	3608.88	6.60	12.36	13.93
^{30}Em		1804.18	5.06	6.10	8.05		1787.00	4.92	5.90	6.65
^{14}N–Em										
^{1}H	9.273	327.80	1.29	1.00	1.29	8.966	313.24	1.11	1.00	1.11
^{12}C	14.892	1109.69	3.64	3.55	4.58	14.843	1093.08	3.52	3.44	3.80
^{14}N	4.281	1198.46	3.83	3.83	4.95	4.273	1182.05	3.71	3.71	4.10
^{16}O	13.145	1284.50	4.00	4.08	5.27	13.135	1268.24	3.88	3.95	4.37
^{32}S	0.0007	1752.96	4.77	5.98	7.74	0.0007	1737.10	4.64	5.77	6.38
^{80}Br	26.770	2718.51	5.72	9.65	12.47	26.926	2702.18	5.57	9.27	10.26
^{127}Ag	31.471	3195.86	6.03	11.08	14.32	31.679	3179.18	5.88	10.64	11.78
^{127}I	0.0010	3476.28	6.25	11.98	15.48	0.0010	3459.40	6.02	11.50	12.72
^{30}Em		1700.72	4.70	5.78	7.48		1684.85	4.56	5.58	6.17
^{12}C–Em										
^{1}H	8.714	288.36	1.26	1.00	1.26	8.411	274.92	1.08	1.00	1.08
^{12}C	14.688	1024.58	3.38	3.38	4.25	14.635	1008.32	3.27	3.27	3.53
^{14}N	4.235	1109.69	3.55	3.68	4.58	4.225	1093.59	3.44	3.52	3.80
^{16}O	13.036	1192.35	3.69	3.87	4.87	13.021	1176.35	3.58	3.74	4.04
^{32}S	0.0007	1643.57	4.36	5.61	7.07	0.0007	1627.77	4.24	5.41	5.84
^{80}Br	27.136	2579.40	5.17	8.94	11.27	27.298	2562.95	5.04	8.58	9.27
^{127}Ag	32.019	3043.56	5.42	10.23	12.89	32.238	3026.71	5.29	9.81	10.60
^{127}I	0.0010	3316.50	5.62	11.04	13.90	0.0010	3299.43	5.41	10.58	11.43
^{30}Em		1593.11	4.30	5.43	6.84		1577.32	4.18	5.23	5.65
p–Em										
^{1}H	2.504	30.27	1.00	1.00	1.00	2.127	24.75	1.00	1.00	1.00
^{12}C	11.315	288.36	1.00	1.26	1.26	11.212	274.92	1.06	1.08	1.08
^{14}N	3.424	327.80	1.00	1.92	1.29	3.401	313.24	1.09	1.11	1.11
^{16}O	10.977	366.84	1.00	1.32	1.32	10.924	351.24	1.11	1.13	1.13
^{32}S	0.0007	597.71	1.00	1.62	1.62	0.0007	575.17	1.22	1.38	1.38
^{80}Br	31.988	1110.90	1.00	2.18	2.18	32.194	1075.71	1.34	1.84	1.84
^{127}Ag	39.593	1375.32	1.00	2.38	2.38	39.943	1334.66	1.38	2.00	2.00
^{127}I	0.0013	1552.30	1.00	2.48	2.48	0.0013	1487.96	1.38	2.11	2.11
^{30}Em		571.05	1.00	1.59	1.59		549.25	1.21	1.35	1.35

which are associated with the reaction systems ^{16}O–Em and ^{12}C–Em, one obtained good agreement with the corresponding experimental data within experimental error. While for the other average values one gets disagreement with the corresponding measured values, but these average values are still nearer to the corresponding experimental values and more realistic than those that are obtained with applying the Gl-I and Gl-II approaches. Furthermore, it is clear that the calculations, which have been done in the framework of these approaches, are near to each other and they deviate from the corresponding experimental data by a noticeable amount. This situation may be refined if one takes into account the above mentioned comments for the calculations of the total-reaction cross sections in accordance with these two approaches.

The different percentages of the reactions, for the following projectiles: ^{32}S, ^{28}Si, ^{24}Mg, ^{22}Ne, ^{16}O, ^{14}N, ^{12}C, and P with each nucleus separated from the emulsion nuclei, have

Table 6. A comparison between the average calculated values of the shower particles multiplicities in the framework of Gl-I and Gl-II approaches and the corresponding experimental data.

		Calculations of Gl-I			Calculations of Gl-II		
Reaction system	$<n_s>^{\text{expt.}}$	$<n_s>$ P P + TP	$<n_s>$ BC	$<n_s>^{\text{theor.}}$	$<n_s>$ P P + TP	$<n_s>$ BC	$<n_s>^{\text{theor.}}$
^{32}S–Em	13.40±0.40 [42]	11.21	14.66	12.94	11.99	14.24	13.12
^{28}Si–Em	11.64±0.34 [43]	10.59	13.67	12.13	11.28	13.28	12.28
	12.90±0.40 [50]						
^{24}Mg–Em	11.09±0.33 [44]	9.85	12.27	11.06	10.53	11.97	11.25
	11.00±0.40 [51]						
^{22}Ne–Em	10.53±0.05 [45]	9.45	11.60	10.53	10.11	11.28	10.70
^{16}O–Em	10.50±0.60 [46]	8.16	9.58	8.87	8.71	9.34	9.03
^{14}N–Em	7.70±0.29 [47]	7.69	8.90	8.30	8.16	8.65	8.41
^{12}C–Em	7.60±0.20 [48]	7.63	8.14	7.12			7.76
	7.80±0.20 [52]						

been calculated and tabulated in the Table 5. In addition, the calculated total-reaction cross sections for these projectiles with the emulsion sample, as the target nucleus of mass number equal to 30 and rms = 3.194 fm., are also tabulated in Table 5. The percentage of this reaction represents the ratio between $\sigma^{\text{ml.}}_{\text{total}-r}$, for each emulsion nuclei, to the summation of $\sigma^{\text{ml.}}_{\text{total}-r}$, for all emulsion nuclei together. On the other hand, the calculations of the average numbers from both the projectile and target participants and from the binary collisions, for the reactions of these projectiles with emulsion nuclei, have been carried out according to the Gl-I and Gl-II approaches and they are tabulated in Table 5. It is clear that the value of the reaction's percentage, the interaction of every projectile with the individual emulsion nuclei depends on the chemical concentration of each one from these nuclei. In addition, one can note that the value of the reaction's percentage, for the interactions of different projectiles with the same emulsion nucleus as: ^{32}S–^{1}H, ^{28}Si–^{1}H, ^{24}Mg–^{1}H.......etc., decreases as the mass number of the projectile decreases, which means that these percentages depend, also, on the mass number of the projectile. At the same time, the values of the projectile participants (PP) and target participants (TP), and the values of participants from binary collisions (BC), for interactions of any projectile being considered with the emulsion nuclei, increases as the mass number of these nuclei increases. On the other hand the values of PP, TP, or BC for the interaction of the different projectiles^{32}S-^{12}C, ^{28}Si-^{12}C, ^{24}Mg-^{12}C...etc. with the same emulsion nucleus decreases as the mass number of the different projectiles decreases. Also, the summations of the values of PP and TP, for reactions such as ^{32}S–^{1}H or ^{28}Si–^{1}H or ^{24}Mg–^{1}H or ^{32}S–^{12}C or ^{28}Si–^{12}C or ^{24}Mg–^{12}C...etc., are usually larger than the corresponding values that are associated with the BC. Thus, one concludes that the values of the projectiles and the target participants besides those ones that are obtained from the binary collisions, depend on the mass numbers of the different projectiles considered as well as depending on the mass number of the individual emulsion nuclei.

Let us once again consider Table 5. Now as an example we shall consider the ^{32}S–Em interaction where we find, according to the Gl-I approach that we have on average 15.34 participants and 12.31 binary collisions for this interaction, to be compared with the corresponding values for proton-induced interaction, which are 2.59 and 1.59, respectively. The two ratios describing the increase or the growth of the amount of the nuclear matter will be 5.92 and 7.74 for the case of participating nucleons and for binary collisions, respectively. Multiplying multiplicities given by the following equation (49):

$$<n_S>_{\text{p}-\text{Em}} = 2.34<n_{\text{ch}}>_{\text{pp}} - 4.12 \tag{19a}$$

by these two ratios, one gets:

$$<n_S>_{^{32}\text{S}-\text{Em}} = 13.85<n_{\text{ch}}>_{\text{pp}} - 24.39 \tag{19b}$$

for the PP and TP participants approach and

$$<n_S>_{^{32}\text{S}-\text{Em}} = 18.11<n_{\text{ch}}>_{\text{pp}} - 31.89 \tag{19c}$$

for the binary collision approach. It is clear from (19a) that the average multiplicities of singly charged relativistic particles in proton–nucleus reactions depend linearly on the charged particle multiplicity in proton–proton interaction at the same energy [28]. Summing the resultant values of (19b) and (19c), one gets the average calculated values of $<n_S>_{^{32}\text{S}-\text{Em}}$ at $E_{\text{Lab.}} = 3.7$ GeV/n. Following the same procedures one gets the other average calculated values of $<n_S>$ and $<n_S>^{\text{theor.}}$ for the different reactions: ^{28}Si–Em, ^{24}Mg–Em, ^{22}Ne–Em, and so on. These average calculated values of $< n_S>$ are compared with the corresponding experimental values as shown in Table 6 [49]. It is clear, from Table 6 that the values of the calculated multiplicities for the participants approach, in the framework of Gl-I and Gl-II, are usually smaller than those that are calculated with the binary collision approach. This means that the expected amount of the shower particles comes from the binary collisions for all the reactions considered above. Also, it is observede that both Gl-I and Gl-II approaches can reproduced the average of the multiplicities successfully for projectiles of mass numbers: $A = 12 \rightarrow 32$.

Moreover, we have drawn, in Figs. 1 and 2, the relations between the average calculated values of the multiplicities for the reaction systems considered, which are given in Table 6, and the corresponding experimental values. The continuous lines, in Figs. 1 and 2, represents the best fit of our considered situations. As a consequence for drawing of these relations we have obtained the following empirical formulae:

Fig. 1. Tthe relation between the average calculated values of the multiplicities for the different reaction systems considered and the corresponding experimental valuesare shown. The continuous line represents the best fit in case of Gl-I approach.

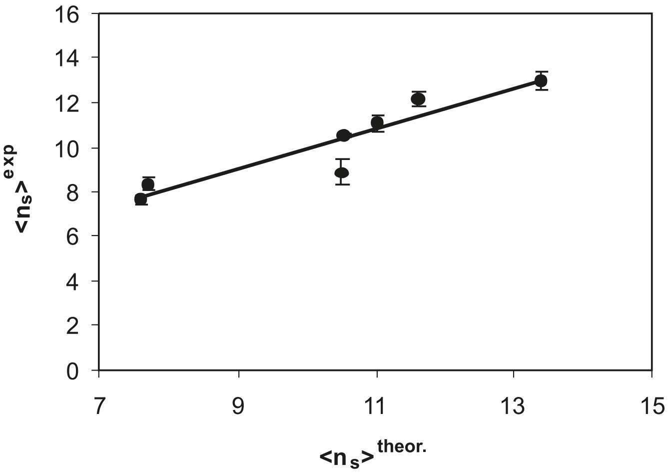

Fig. 2. The relation between the average calculated values of the multiplicities for the different reaction systems considered and the corresponding experimental values are shown. The continuous line represents the best fit in case of Gl-II approach.

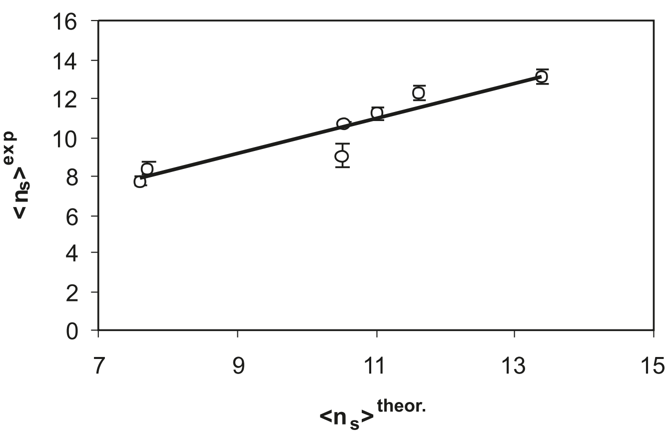

$$<n_S>^{\mathrm{expt.}} = 0.8984<n_S>^{\mathrm{theor.}} + 0.9253 \tag{20a}$$

for the calculations in the framework of the Gl-I approach and

$$<n_S>^{\mathrm{expt.}} = 0.9090<n_S>^{\mathrm{theor.}} + 0.9677 \tag{20b}$$

for the calculations in accordance with the Gl-II approach. It should be mentioned that these empirical formulae are valid for projectiles of mass numbers in the range $12 \leq A \leq 32$. On the other hand, and as shown in Figs. 1 and 2, we can conclude that, the predicted values for $<n_S>$ of these two approaches are adequate encouraged when compared with the corresponding experimental data.

For more investigation the averaged calculated values of the multiplicity for the interaction of the different projectiles with the standard emulsion ($<n_s>^{\mathrm{theor.}}$), in the framework of the Gl-I and Gl-II approaches, and the corresponding experimental one ($<n_s>^{\mathrm{expt.}}$), are plotted together versus the quantity $(A_p^{1/3} + A_T^{1/3})$ as shown in Figs. 3 and 4, respectively. It should be noticed that A_T represents the mass number of the averaged target nucleus of the emulsion sample as a whole. In addition, the multiplicity of both the particle participants ($<n_s>^{\mathrm{part.}}$) and the one which is associated with the binary

Fig. 3. The best linear fit for the average calculated values of the multiplicities ($< n_s >^{\mathrm{theor.}}$), in the framework of the Gl-I approach, for the different reaction systems considered (continuous line) and the corresponding experimental data (solid circles) are plotted versus the quantity $(A_P^{1/3} + A_T^{1/3})$. Also the multiplicity for both PP + TP ($< n_s >^{\mathrm{part.}}$), the dash–dot line, and for BC ($< n_s >^{\mathrm{BC}}$), the broken line, are shown.

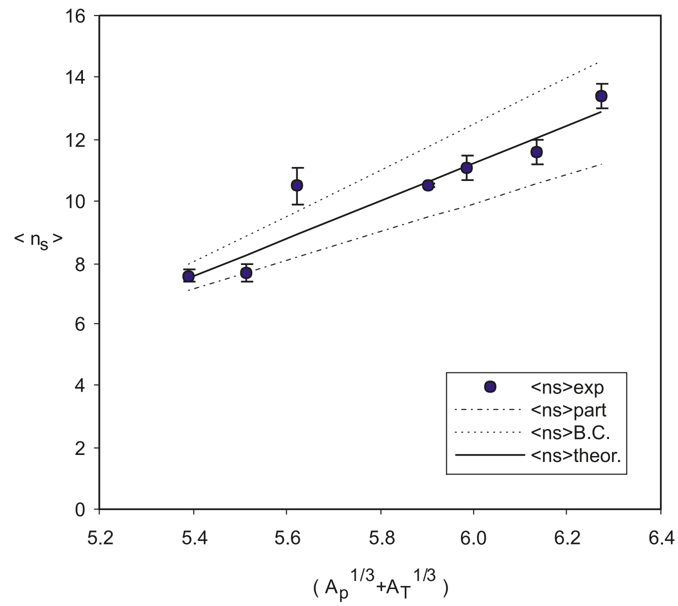

Fig. 4. The best linear fit for the average calculated values of the multiplicities ($< n_s >$), in the framework of Gl-II approach, for the different reaction systems considered (continuous line) and the corresponding experimental data (solid circles) are plotted versus the quantity $(A_P^{1/3} + A_T^{1/3})$. Also the multiplicity for both PP + TP ($< n_s >_{\mathrm{part.}}$) , the dash–dot line, and for BC ($< n_s >_{\mathrm{B.C.}}$), the broken line, are shown.

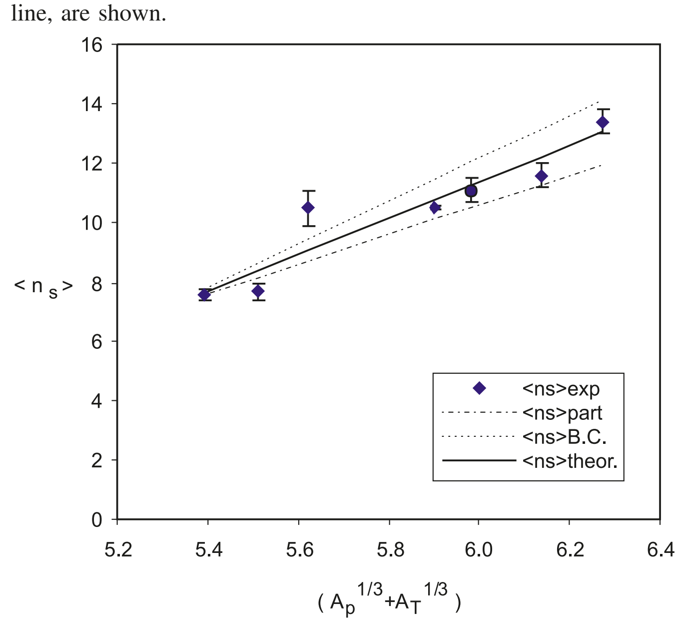

collisions ($<n_s>^{BC}$) are also plotted together versus the quantity $(A_p^{1/3} + A_T^{1/3})$ in Figs. 3 and 4.

At the same time we have obtained the following empirical formula:

$$<n_s>^{expt.} = 5.9000(A_P^{1/3} + A_T^{1/3}) - 24.063 \tag{21}$$

which relates the different values of $<n_s>^{expt.}$ for the following interactions: ^{32}S–Em, ^{28}Si–Em, ^{24}Mg–Em,….etc., and the corresponding values of the quantity $(A_p^{1/3} + A_T^{1/3})$. This equation is valid for the calculations in the framework of both Gl-I and Gl-II approaches. Other empirical formulae have been obtained. These formulae relate, in case of Gl-I approach, the multiplicity of the particle participants (PP + TP), the multiplicity of the binary collision, and the average calculated values of the multiplicities for all considered reaction systems and the corresponding values of the quantity $(A_p^{1/3} + A_T^{1/3})$:

$$<n_s>^{part.} = 4.6306(A_P^{1/3} + A_T^{1/3}) - 17.853 \tag{22a}$$

$$<n_s>^{BC} = 7.4441(A_P^{1/3} + A_T^{1/3}) - 32.154 \tag{22b}$$

and

$$<n_s>^{theor.} = 6.0388(A_P^{1/3} + A_T^{1/3}) - 25.010 \tag{22c}$$

respectively. At the same time we have obtained, in case of Gl-II approach, the following empirical formulae for the same quantities mentioned before:

$$<n_s>^{part.} = 4.9910(A_P^{1/3} + A_T^{1/3}) - 19.343 \tag{23a}$$

$$<n_s>^{BC} = 7.2092(A_P^{1/3} + A_T^{1/3}) - 31.087 \tag{23b}$$

and

$$<n_s>^{theor.} = 6.1001(A_P^{1/3} + A_T^{1/3}) - 25.211 \tag{23c}$$

Also it should be mentioned, here, that these empirical formulae are valid for the projectile's mass number: $12 \leq A_p \leq 32$. It is clear that the numerical values of the intersection coefficients in case the empirical formulae of $<n_s>^{theor.}$ are always half the values with respect to those obtained in case of $<n_s>^{part.}$ and $<n_s>^{BC}$ together.

As a final conclusion, one can say that both the Gl-I and Gl-II approaches have reproduced, successfully, the multiplicities of the shower particles, which are produced in all the reaction systems considered, in spite of this these approaches have not reproduced the corresponding total-reaction cross sections successfully. Also one can say that both the projectile and target participants except those that are obtained from binary collisions are mass-number (target and projectile) dependent. This means that the multiplicities of the shower particles are also mass-number (target and projectile) dependent as well as being energy dependent as we concluded in our previous article [24].

References

1. R.G. Glauber. Lectures on theoretical physics. Vol. 1. Inter-Science, New-York. 1958.
2. P.J. Karol. Phys. Rev. D: Part. Fields, **26**, 1497 (1975).
3. A.J. Cole, W.D.M. Rae, M.E. Branden, A. Dacal, B.G. Harvey, R. Legrain, M.J. Murphy, and R.G. Stokstad. Phys. Rev. Lett. **47**, 1705 (1981). doi:10.1103/PhysRevLett.47.1705.
4. M. Buenerd, A. Lounis, J. Chauvin, D. Lebrun, P. Martin, G. Duhamel, J.C. Gondrand, and P. de Saintgnon. Nucl. Phys. **A424**, 313 (1984). doi:10.1016/0375-9474(84)90186-6.
5. S. Kox, A. Gamp, R. Cherkaoui, A.J. Cole, N. Longequeue, J. Menet, C. Perrin, and J.B. Viano. Nucl. Phys. **A420**, 162 (1984). doi:10.1016/0375-9474(84)90663-8.; S. Kox, A. Gamp, C. Perrin, J. Arvieux et al. Phys. Rev. C: Nucl. Phys. **35**, 1678 (1987) and references therein.
6. W.Q. Shen, B. Wang, J. Feng, W.L. Zahan, Y.T. Zhu, and E.P. Feng. Nucl. Phys. **A491**, 130 (1989).
7. R.E. Warner and G.N. Felder. Phys. Rev. C: Nucl. Phys. **42**, 2252 (1990).
8. M.S. Hussein, R.A. Rego, and C.A. Bertulani. Phys. Rep. **201**, 279 (1991). doi:10.1016/0370-1573(91)90037-M.
9. C.E. Aguiar, F. Zardi, and A. Vitturi. Phys. Rev. C: Nucl. Phys. **56**, 1511 (1997).
10. M.Y.H. Farag. Eur. Phys. J. A, **12**, 405 (2001). doi:10.1007/s10050-001-8664-2.
11. M.S.M. Nour El-Din. Egypt. J. Phys. **34**, 139 (2003); Egypt. J. Phys. **35**, 509 (2004).
12. A.Sh. Ghazal, M.S.M. Nour El-Din, and M.Y.M. Hassan. Eur. Phys. J. A, **19**, 221 (2004). doi:10.1140/epja/i2003-10101-8.
13. M.A. Alvi. Nucl. Phys. **A789**, 73 (2007).
14. J. Chauvin, D. Lebrun, A. Lounis, and M. Buenerd. Phys. Rev. C: Nucl. Phys. **28**, 1970 (1983).
15. A. Vitturi and F. Zardi. Phys. Rev. C: Nucl. Phys. **36**, 1404 (1987).
16. S.M. Lenzi, A. Vitturi, and F. Zardi. Phys. Rev. C: Nucl. Phys. **40**, 2114 (1989).
17. S.K. Charagi and S.K. Gupta. Phys. Rev. C: Nucl. Phys. **46**, 1982 (1990).
18. A.Y. Abul-Magd and M. Talib Ali-Alhenai. Nuovo Cimento Soc. Ital. Fis. A, **110**, 1281 (1997).
19. X. Cai, J. Feng, W. Shen, Y. Ma, J. Wang, and W. Ye. Phys. Rev. C: Nucl. Phys. **58**, 572 (1998).
20. M.S.M. Nour El-Din. Egypt. J. Phys. **39**, 143 (2008).
21. M.H. Cha. Phys. Rev. C: Nucl. Phys. **46**, 1026 (1992).
22. S.K. Charagi. Phys. Rev. C: Nucl. Phys. **48**, 452 (1993); **51**, 3521 (1995).
23. M.K. Hegab and J. Hufner. Phys. Lett. **105B**, 103 (1981); Nucl. Phys. **A384**, 353 (1982).
24. M.S.M. Nour El-Din and M.E. Solite. Can. J. Phys. **86**, 1209 (2008). doi:10.1139/P08-043.
25. D. Kang, S.H. Ling, and K. Young. Phys. Rev. D: Part. Fields, **31**, 31 (1985).
26. K. Fialkowski. Phys. Lett. **169B**, 436 (1986).
27. M.K. Hegab, M.T. Hussein, and N.M. Hassan. Z. Phys. A: Atomic Nuclei, **336**, 345 (1990) doi:10.1007/BF01292867.; M.K. Hegab, M.T. Hussein, and N.M. Hassan. J. Phys. G: Nucl. Part. Phys. **16**, 607 (1990). doi:10.1088/0954-3899/16/4/011.
28. M.I. Adamovich, M.M. Aggarwal, Y.A. Alexandrov et al. Phys. Rev. Lett. **227**, 285 (1987); M.I. Adamovich, M.M. Aggarwal, Y.A. Alexandrov et al. Phys. Rev. Lett. **62**, 2801 (1989). doi:10.1103/PhysRevLett.62.2801.; M.I. Adamovich, M.M. Aggarwal, Y.A. Alexandrov et al. Phys. Lett. **223B**, 262 (1989). doi:10.1016/0370-2693(89)90250-5.; M.I. Adamovich, M.M. Aggarwal, Y.A. Alexandrov et al. Phys. Rev. Lett. **69**, 745 (1992). doi:10.1103/PhysRevLett.69.745.; M.I. Adamovich, M.M. Aggarwal,

Y.A. Alexandrov et al. Z. Phys. C, **56**, 509 (1992) doi:10.1007/BF01474723.; EMU01 Collaboration. M.I. Adamovich, M.M. Aggarwal, Y.A. Alexandrov et al. Nucl. Phys. **A593**, 535 (1995); M.I. Adamovich, M.M. Aggarwal, Y.A. Alexandrov et al. Z. Phys. A, **358**, 337 (1997). doi:10.1007/s002180050337.
29. S. El-Sharkawy, M.K. Hegab, M.M. Sherif, O.M. Osman, and M.A. Jilany. Z. Phys. A, **346**, 237 (1993). doi:10.1007/BF01306084.
30. M. Nabil Yasin, M.M. Sherif, S.M. Abd El-Halim, and M.A. Jilany. Sov. Phys. JETP, **84**, 635 (1997). doi:10.1134/1.558193.
31. M.A. Jilany. Eur. Phys. J. A, **22**, 471 (2004). doi:10.1140/epja/i2004-10051-7.
32. M.E. Solite. Egypt. J. Phys. **39** (2008).
33. S.K. Charage and S.K. Gupta. Phys. Rev. C: Nucl. Phys. **41**, 1610 (1990).
34. P.J. Karol. Phys. Rev. C: Nucl. Phys. **46**, 1988 (1992).
35. E.H. Esmael, M.S.M. Nour El-Din, and M.Y.M. Hassan. Egypt. J. Phys. **36**, 161 (2004).
36. S.K. Gupta and P. Shukla. Phys. Rev. C: Nucl. Phys. **52**, 3212 (1995).
37. I.S. Gradshteyn and I.M. Ryzhik. Table of integration, series and product. English Edition. Academic Press Inc., New York, London, Toronto, Sydney, and San Francisco. 1980.
38. J. Friedrich and N. Voegler. Nucl. Phys. **A373**, 192 (1982). doi:10.1016/0375-9474(82)90147-6.
39. V. Franco and G.K. Varma. Phys. Rev. C: Nucl. Phys. **18**, 349 (1978).
40. H. De Vries, C.W. De Jager, and C. De Vries. At. Data Nucl. Data Tables, **36**, 495 (1987). doi:10.1016/0092-640X(87)90013-1.
41. W.H. Barkas. Nuclear research emulsion. Academic Press, New York and London. 1963. p. 73.
42. A. Abdelsalam, E.A. Shaat, N. Ali-Mossa, Z. Abou-Mousa, O.M. Osman, N. Rashed, W. Osman, B.M. Badawy, and E. El-Falaky. J. Phys. G: Nucl. Part. Phys. **28**, 1375 (2002). doi:10.1088/0954-3899/28/6/317.
43. M.A. Jilany. Nucl. Phys. **A579**, 627 (1994). doi:10.1016/0375-9474(94)90926-1.
44. Al.-B.M. Abd El-Daim. Ph.D. thesis, Faculty of Science (Sohag), Assiut University. 1991.
45. Alma-Ata-Bucharest-Dubna-Dushambe-Ervan-Kosice-Krakow-Leningrad-Moscow-Rzez-Tashkant-Tbilist Ulan-Bator collaboration. Sov. J. Nucl. Phys. **451**, 78 (1987).
46. H.H. Hekman, D.E. Greiner, P.J. Lindstrom, and H. Shwe. Phys. Rev. C: Nucl. Phys. **17**, 1735 (1978); V.A. Antonchik, et al. Sov. J. Nucl. Phys. **39**, 774 (1984).
47. G.D. Westfoll, L.W. Wilson, P.J. Lindstrom, H.J. Crawford, D.E. Greiner, and H.H. Hekman. Phys. Rev. C: Nucl. Phys. **19**, 1309 (1979).
48. A. El-Naghy and V.D. Toneev. Z. Phys. A, **298**, 55 (1980). doi:10.1007/BF01416028.
49. B. Anderson, I. Otterlund, and E. Stenlund. Phys. Lett. **84B**, 469 (1979).
50. M.I. Adamovich et al. (EMUOI Collaboration). Dubna Preprint, El-92–569. 1992.
51. A. El-Naghy, M.T. Ghoniem, S. El-Sharkawy, and Al-B.M. Abd El-Daim. Nucl. Sci. J. **26**, xx (1989).
52. A. Abdelsalam. Dubna Preprint El-81–623. 1981; B.V. Ameeva et al. Dubna Preprint El-89–560. 1989.